SAND2016-7297R

Analysis and screening tools for ducted fuel injection (DFI) experiments

Daniel Ruth
Sandia National Laboratories, Livermore, CA

July 26, 2016

Abstract

Methods for processing recorded data and efficiently screening experimental results from ducted fuel injection (DFI) experiments for soot mitigation in diesel engines are described. Specifically, a method for locating the spray tip in natural luminosity movies is detailed. DFI implementations are analyzed and are seen to significantly lower soot levels.

1 Introduction

Ducted fuel injection (DFI) is an in-cylinder technique for lowering the quantity of soot produced by diesel engines, wherein a portion of the fuel spray is constrained by a circular duct that enhances fuel/air mixing and leads to leaner lifted-flame combustion (LLFC). LLFC is an advanced combustion strategy in which the equivalence ratio at the diffusion flame's lift-off location is sufficiently low (≤ 2) such that little to no soot is formed [1]. Figure 1 shows a schematic of DFI combustion.

Previous studies have achieved LLFC through the use of combustion strategies that decrease the equivalence ratio at the liftoff length by enabling greater entrainment before combustion [1], and through the use of oxygenated fuels [2].

Two investigations into DFI at Sandia have suggested that DFI is a viable method for attaining LLFC. Results from these studies and the methods with which they are analyzed are presented in this paper.

2 Diagnostic analysis

2.1 Experimental setup

Experiments were conducted in Sandia's constant-volume combustion vessel (CVCV). The temperature, density, and gas composition of the vessel at the time of the combustion event can be controlled to simulate a range of diesel engine conditions [3]. In the two DFI investigations analyzed (DFI1 and DFI2), DFI geometries were tested over a range of temperatures (800 K to 1200 K), two ambient densities (14.8 and 22.8 $\mathrm{kg/m^3}$), and two oxygen mole fractions (15% and 21%, simulating EGR and no-EGR operation). Injection parameters closely matched ECN Spray A conditions [4].

The duct parameters that were varied include the duct material, length L, inside diameter D, distance from the injector G, and contour of the duct inlet and outlet.

The CVCV and equipment used for obtaining data are shown in Figure 2. DFI data taken in the CVCV over investigations DFI1 and DFI2 include natural luminosity (NL) recordings of hot soot, chemiluminescense (CL) recordings of electronically excited hydroxyl (OH^*) radicals (to locate high-temperature reaction regions), diffused backlit illumination (DBI) recordings to quantify soot mass, photodiode measurements of NL, and vessel pressure measurements. With these data, spray penetration, soot mass, rate of heat release, lift-off length, and pressure rise rate are computed over the duration of each combustion event. Additionally, data for each case are reduced to scalar values including average soot levels, lift-off length, ignition delay, and soot reduction in comparison to the free-jet baselines.

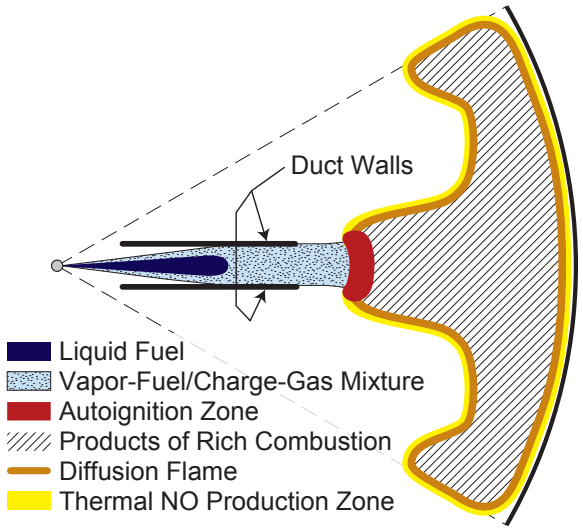

Figure 1: Schematic of diesel combustion with DFI.

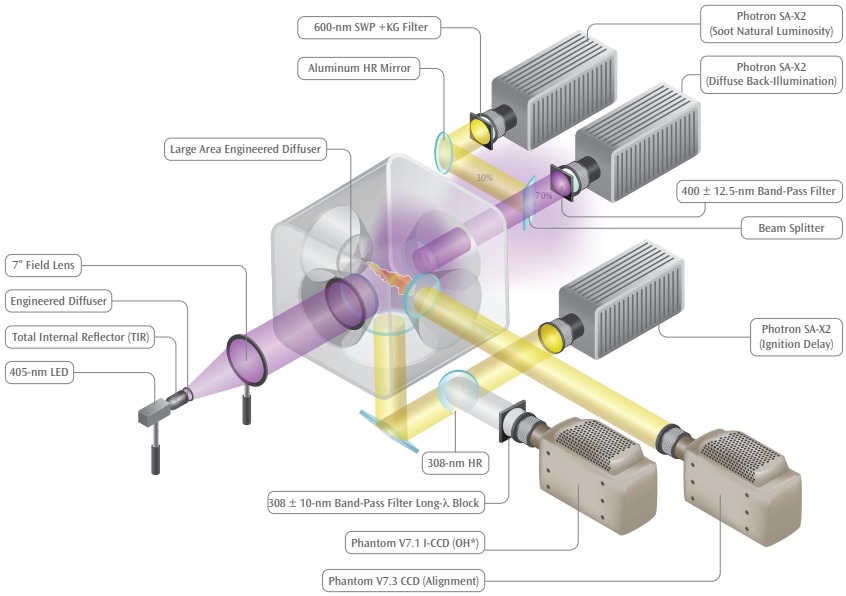

Figure 2: Constant-volume combustion vessel and diagnostic equipment setup for DFI2 experiments.

2.2 Spray penetration analysis

The traditional gradient method of tip location identification, in which the tip is defined as the axial location of the most negative axial NL gradient, was found to be insufficient for extracting the spray penetration from NL movies. In its place, a method involving a "tip-isolating image" has been implemented.

2.2.1 Reducing NL movie to 2-d t-z image

A background subtraction (with the background being the average of the first few frames before start of injection) is first performed on each frame of the NL movie.

Then for each frame, the average pixel value at each point along the injection axis is computed by averaging the middle portion (near the injection centerline) of each row (when the frame is rotated such that the spray is injected upwards). The columns of axial intensity for each frame are aligned side-by-side, such that the horizontal axis represents time and the vertical axis represents axial distance, creating image I. The intensity at each pixel in I is the average pixel intensity at that axial position in the corresponding frame. Figure 3 shows this axial intensity image I for a free spray case.

Figure 3: Axial intensity image I for a free spray case.

The desired spray penetration curve, originating at the bottom left corner, is discernible in the early luminous period of the spray, but once the spray tip passes beyond a certain axial position the signal weakens due to the upstream region's higher luminosity.

2.2.2 Constructing tip-isolating image

To locate the tip in the region beyond this point, a tip-isolating image is constructed considering that near the tip, the axial gradient of I should be very negative, the temporal gradient of I should be very positive, the mean of the downstream intensities should be small, and the mean of the upstream intensities should be large. This gives conditions near the tip at time t:

$$-\frac{\partial I_{z,t}}{\partial z} >> 0 \tag{1}$$

$$\frac{\partial I_{z,t}}{\partial t} >> 0 \tag{2}$$

$$\text{adj}\left(\frac{\sum_{z}^{z_{\text{end}}} I_{z,t}}{z_{\text{end}} - z}\right) \approx 0 \tag{3}$$

$$\text{adj}\left(\frac{\sum_{z_{\text{noz}}}^{z} I_{z,t}}{z - z_{\text{noz}}}\right) >> 0 \tag{4}$$

where *adj* represents a constant value added to the matrix such that the minimum entry is 1, which is done to correct for background-subtraction issues that may cause some entries to be 0 or negative.

The tip-isolating image T is created by taking the element-wise product of the three matrices which are large near the tip and dividing by the one which is small near the tip,

$$T = -\frac{\partial I}{\partial z} \cdot \frac{\partial I}{\partial t} \cdot \text{adj}\left(\frac{\sum_{z_{\text{noz}}}^{z} I}{z - z_{\text{noz}}}\right) \Big/ \text{adj}\left(\frac{\sum_{z}^{z_{\text{end}}} I}{z_{\text{end}} - z}\right). \tag{5}$$

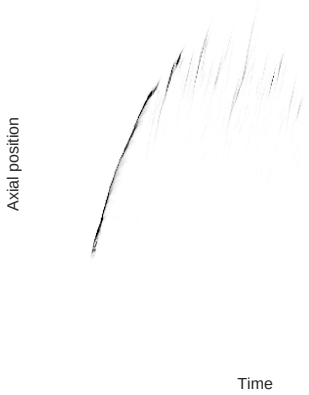

Figure 4: Tip-isolating image T for the case shown in Figure 3.

The tip-isolating image T for the axial intensity image I shown in Figure 3 is shown in Figure 4. Note the more concentrated signal near the jet tip and weaker signal in the upstream regions which are very luminous in Figure 3. After the tip passes a certain axial position, the signal upstream of the tip in T is still stronger, but by a small enough degree that the filtering algorithm described in the following section is able to locate the tip.

2.2.3 Searching for the spray tip

The search for the tip in a frame taken at time t is done by considering the column of T corresponding to this frame, denoted T_t. At each frame, a number of restrictions are applied:

1. Values in T_t below a certain threshold are set to 0. This way, any frame that has just noise and no significant values will not have a tip location selected. The value of this threshold will depend heavily on camera settings employed and should be determined on a study-by-study basis.

2. If possible, a linear fit is applied to the previous n (typically 5) tip locations in t-z space. Two lines are then placed in T through the most distant of the n tips, with slopes that are some factor of the fit's slope m (e.g., $0.5 \cdot m$ and $2 \cdot m$). The search for the tip in the frame of interest is limited to the pixels between those at which the two lines cross the column T_t. This prevents the algorithm from choosing a point far from previously found locations as the tip.

3. Pixels upstream of the maximum calculated tip location from the previous 10 frames are set to 0 to prevent the algorithm from choosing a point behind the tip that happens to have a strong signal.

Once these filters are applied, a set of possible tip locations in T_t is constructed by identifying the points that may contain the tip location: these are the points whose values are at least some portion of the way between the minimum and maximum remaining values in T_t. The point selected as the tip is the farthest-downstream of these points, and the process is repeated for the following frames.

A comparison between the gradient method and tip-isolating method is shown in Figure 5, with the results of each overlaid on the tip-isolating image.

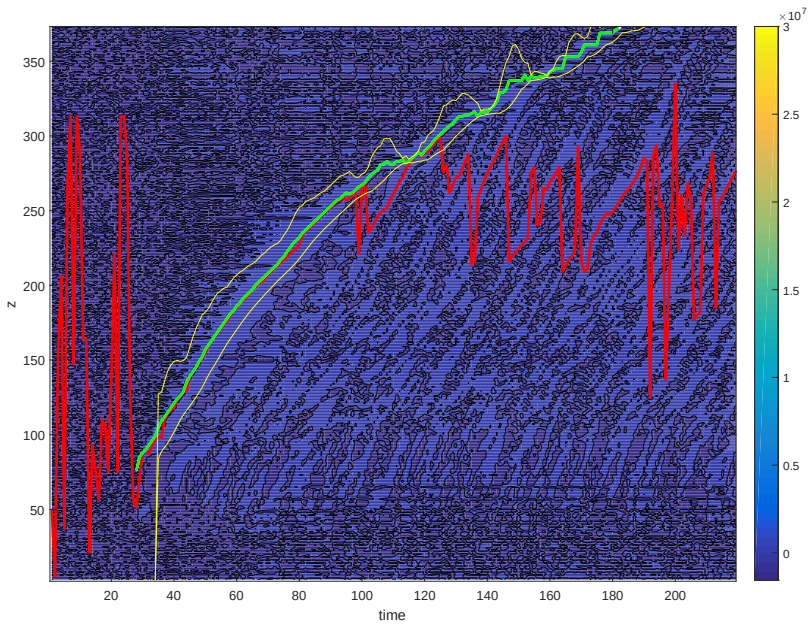

Figure 5: Portion of a tip-isolating image T in the background with the tip locations as found by the gradient method (red) and tip-isolating image method (green). Regions containing a strong signal (colored green and yellow) are largely covered by the superimposed plots.

3 Screening tools

To facilitate the screening of the 60+ DFI conditions that were tested in which 8 parameters were varied and 10+ diagnostics and metrics were recorded or computed, a Matlab utility with an Excel user interface was developed to create "stacked" time plots of vector data and scalar plots of computed metrics. Additionally, a code to create comparison movies of experimental data was developed.

3.1 Plotters

The plotting tools allow the user to select experimental conditions and plot their vector and scalar data together. Selection of the cases to include in the plots is done by specifying the experimental conditions that must be satisfied for inclusion in the plot. This could be, for example, "all cases for which $T = 900\,\mathrm{K}$ and $L = 6$ or $8\,\mathrm{mm}$."

After specifying the conditions for inclusion on the plots, the user specifies which variables will control the color, line style, and line width of the included cases.

Finally, the user specifies which recorded data to show. For the vector data, the user specifies which series to include and the organization of the plots on which they are shown. For the scalar data, the user specifies which variables are to be shown on the x and y axes, and how the datapoints should be grouped, or connected by lines. The script allows for two "grouping" methods to be identified. For each method, cases which have identical values of a set of parameters specified by the user will be connected by lines. The order in which the points are connected by lines is determined by the cases' values of a certain parameter that the user selects as the "sorting" variable for that grouping. When any of the parameters by which cases are grouped are also parameters that determine cases' colors, line styles, or line widths, the lines connecting the points in that group will be assigned that property.

The workflow for the plotting tools involves specifying the above-described data in an Excel spreadsheet. This spreadsheet is used to store the commands for creating each plot for a study. Next, the user runs a

Matlab script that reads in the Excel commands and automatically selects the cases which are to be included, assigns them the appropriate identifying parameters, and creates the vector and scalar plots.

3.2 Movie diagnostic comparisons

To further facilitate experimental data analysis, a Matlab script was developed to create comparison movies of experimental runs, in which movies for a ducted spray and the corresponding free spray run are shown side-by-side, and recorded vector data for the two cases are plotted together. Movies are "stacked" and aligned spatially. This can reveal qualitative information not apparent in the vector or scalar data and serves as a means for efficiently evaluating processed data.

A screenshot of the movie produced comparing a free-spray and ducted spray at 1000 K, 22.8 kg/m^3, and 21.0 % O_2 is shown in fig. 6. The difference in soot is apparent when comparing the NL and DBI images between the two cases.

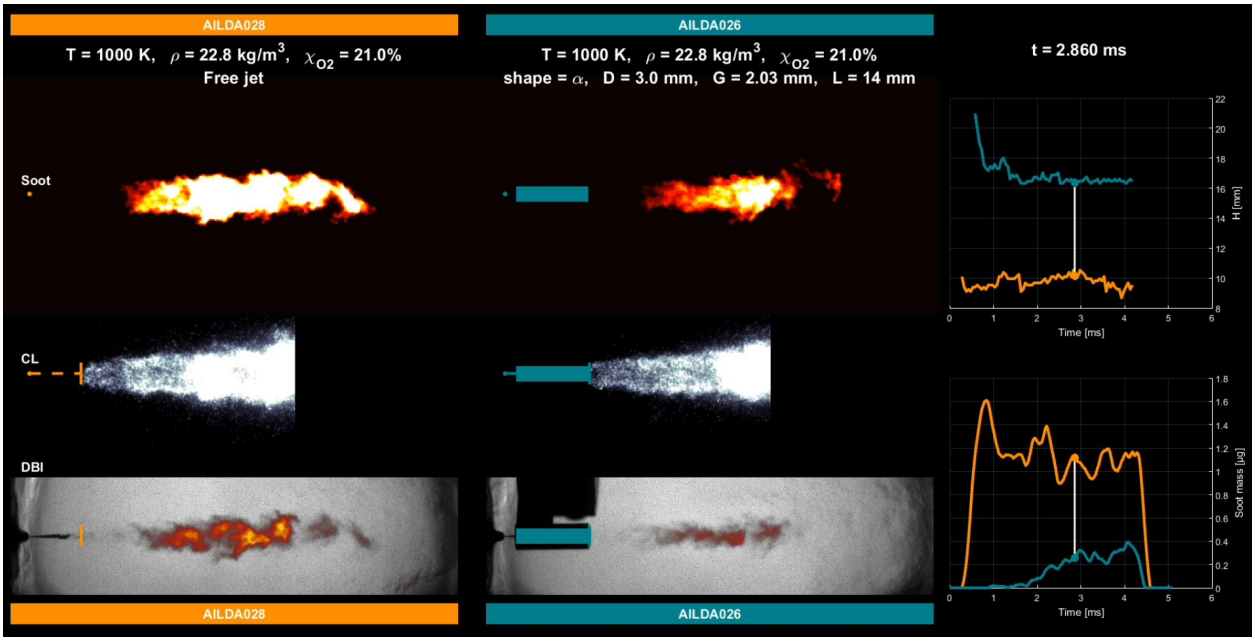

Figure 6: Screenshot of screening movie comparing free-spray (left, orange) and ducted (right, green) cases at 1000 K, 22.8 kg/m^3 and 21.0 % O_2.

4 Results

4.1 Free spray baselines

In the second DFI investigation, DFI2, free sprays were investigated at temperatures of 850 K to 1200 K and ambient oxygen concentrations of 15 % and 21 % by volume. Results are shown in fig. 7. Vector and scalar data shown for the 21 % oxygen cases are the averages of three runs taken at those conditions

More soot is seen with the lower oxygen content, which is used to simulate exhaust gas recirculation (EGR) conditions. For a given amount of ambient gas entrained into a spray upstream of the lift-off length H, higher ambient oxygen contents will lead to lower local equivalence ratios in the spray, since a higher portion of the entrained gas is oxidizer. Thus, the spray in the 21 % case is more capable of approaching LLFC conditions, all other parameters being equal.

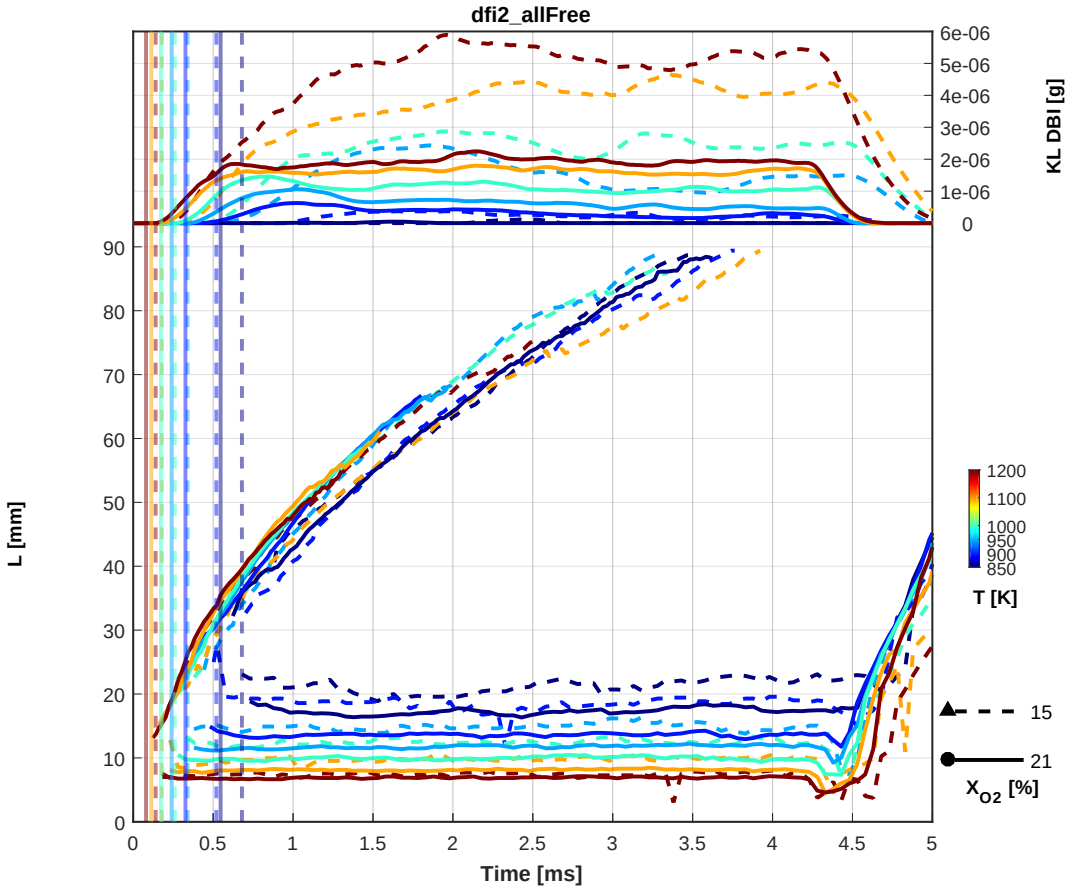

Figure 7: Comparison between oxygen contents for free sprays with $\rho_a = 22.8\,\mathrm{kg/m^3}$. Vertical lines indicate ignition delay as determined from the highly-sensitive Ignition Delay camera shown in Figure 2.

4.2 Soot mitigation via DFI

Figures 8 to 10 show vector and scalar data for a simple DFI geometry (a cylindrical duct positioned 2.03 mm from the injector and with a length and diameter of 14 mm and 3 mm, respectively) and the corresponding free spray baselines. The presence of the duct lowers soot to undetectable levels for ambient temperatures of 900 K and 950 K and provides significant reductions at higher temperatures. Both the ignition delay and lift-off length are greater for ducted sprays.

Lift-off lengths are consistently higher for ducted sprays than they are for free sprays; however, the increase in lift-off length is less than the length of the duct. Results from McQuaid [5], who investigated confined sprays, suggest that entrainment in the region of the spray between the entrance of the duct and the point of impingement on the inner walls of the duct is not significantly impacted by the presence of the duct. Thus, entrainment of hot gas into the spray, the rate of which impacts the lift-off length, may not be fully restricted inside the entire duct.

One factor that complicates any conclusions drawn about the duct's impact on entrainment from the changes in lift-off length is the dependence of entrainment rate on a spray's fuel and velocity profiles [6]. The efficacy of the duct in lowering soot is believed to result from its enhancement of the fuel/air mixing. Such mixing impacts the fuel and velocity distributions in the spray, which in turn impact the downstream ignition and combustion characteristics of the spray.

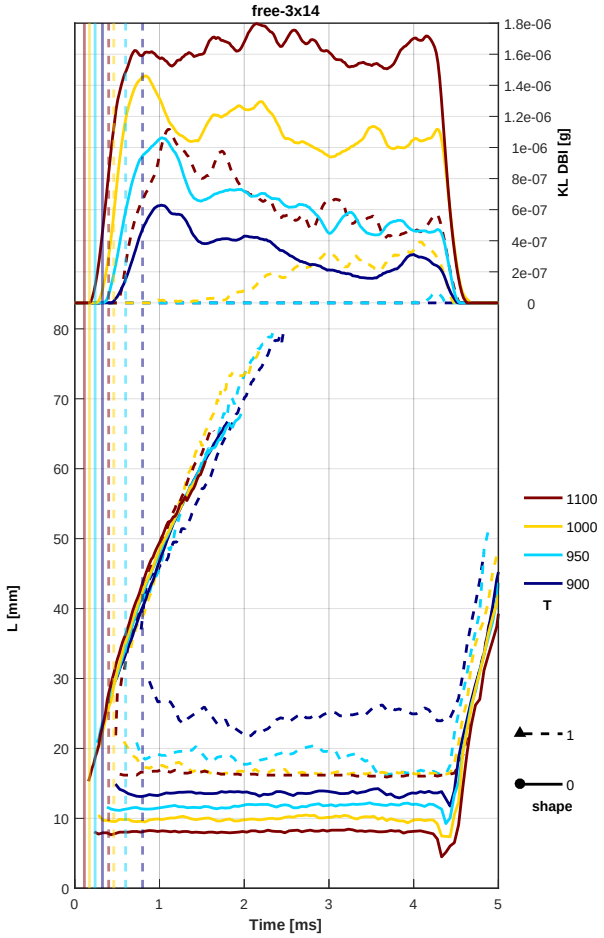

Figure 8: Lift-off length, spray penetration, and soot mass as a function of time for free spray (solid lines) and ducted (dashed lines) cases. Ignition delays are shown as vertical lines.

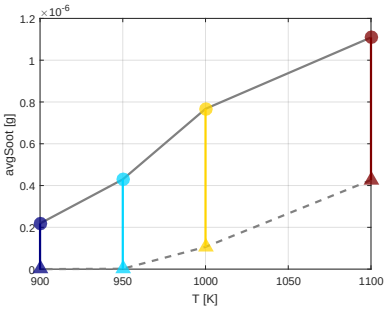

Figure 9: Soot mass as a function of ambient temperature for free spray (solid line) and ducted (dashed line) cases. Legend is the same as shown in Figure 8.

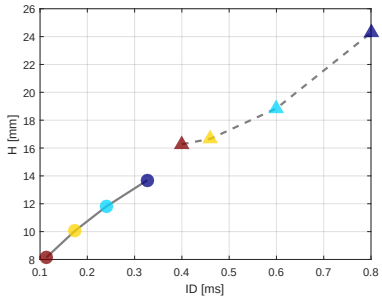

Figure 10: Lift-off length as a function of ignition delay for free spray (solid line) and ducted (dashed line) cases. Legend is the same as shown in Figure 8.

5 Conclusions

The developed data processing and screening tools allow for the efficient analysis of CVCV DFI experimental results. These tools can be used to develop an understanding of the mechanisms behind DFI's efficacy, and future investigations into DFI will be facilitated by these tools.

DFI was seen to eliminate soot at lower temperatures and mitigate soot levels at higher temperatures, where more soot tends to be produced. Future work should quantify the mixing characteristics inside the duct and possibly determine how the duct impacts entrainment over different regions of the spray.

Acknowledgements

The author thanks Dr. Charles Mueller and Dr. Ryan Gehmlich for their guidance on this project and their mentorship throughout the summer.

This work was supported in part by the U.S. Department of Energy, Office of Science, Office of Workforce Development for Teachers and Scientists (WDTS) under the Science Undergraduate Laboratory Internships

Program (SULI).

Sandia National Laboratories is a multi-program laboratory managed and operated by Sandia Corporation, a wholly owned subsidiary of Lockheed Martin Corporation, for the U.S. Department of Energy's National Nuclear Security Administration under contract DE-AC04-94AL85000.

References

[1] C. J. Polonowski, C. J. Mueller, C. R. Gehrke, T. Bazyn, G. C. Martin, and P. M. Lillo, "An experimental investigation of low-soot and soot-free combustion strategies in a heavy-duty, single-cylinder, direct-injection, optical diesel engine," *SAE Int. J. Fuels Lubr.*, vol. 5, no. 1, pp. 51–77, 2011.

[2] R. K. Gehmlich, C. E. Dumitrescu, Y. Wang, and C. J. Mueller, "Leaner lifted-flame combustion enabled by the use of an oxygenated fuel in an optical CI engine," *SAE Int. J. Engines*, vol. 9, 04 2016.

[3] D. L. Siebers, "Liquid-phase fuel penetration in diesel sprays," in *SAE Technical Paper*, SAE International, 02 1998.

[4] "Engine combustion network." http://www.sandia.gov/ecn/cvdata/targetcondition/spraya.php.

[5] J. McQuaid, "Air entrainment into bounded axisymmetric sprays," *Proceedings of the Institute of Mechanical Engineers*, vol. 189, pp. 197–202, may 1975.

[6] M. Musculus and K. Kattke, "Entrainment waves in diesel jets," *SAE International*, vol. 2009-01-1355, 2009.